A Simple Route from Monomeric Nanofibers to Zinc Oxide/Zinc Sulfide Nanoparticle/Polymer Composites through the Combined Use of γ-irradiation Polymerization, Gas/Solid Reaction and Thermal Decomposition

Shiao-Wei Kuo,*,† Yao-Chu Chung,‡ Kwang-Un Jeong,§ and Feng-Chih Chang*,‡

Department of Materials and Optoelectronic Science, Center for Nanoscience and Nanotechnology, National Sun Yat-Sen University, Kaohsiung, Taiwan, Institute of Applied Chemistry, National Chiao Tung University, Hsinchu, Taiwan, and Department of Polymer-Nano Science and Technology, Chonbuk National University, Jeonju 561-756, Korea

Received: June 12, 2008; Revised Manuscript Received: August 15, 2008

We report a simple route to hierarchical zinc oxide/zinc sulfide (ZnO/ZnS) nanoparticle/polymer nanofiber structures through self-assembly of zinc dimethacrylate ($Zn(MA)_2$) in water/ethanol solution. The water clusters in formed around $Zn(MA)_2$ would undergo hydrogen-bonding interactions to create a supramolecular structure and then form the construction of three-dimensional nanofibers and random networks. These monomeric $Zn(MA)_2$ nanofibers are converted into ZnO or ZnS nanoparticle/polymer nanofiber composites through a combination of γ-irradiated polymerizations and in situ thermal decomposition or H_2S gas/solid reactions, respectively. The carboxylic ion groups of P−$Zn(MA)_2$ remained bonded to zinc ions on the particles' surfaces after thermal decomposition or the reaction with H_2S. The compact polymer network prevented the ZnO or ZnS nanoparticles from aggregating to eliminate the defects. High-resolution transmission electron microscopes indicate that ZnO and ZnS particles are highly crystallized with a size of 3−7 nm. This is a simple approach to produce nanoparticle in polymer nanofibers. This preparation method can potentially be extended to other polymer matrices containing different metal ions.

Introduction

One-dimensional (1D) nanostructures, such as nanowires, nanofibers, nanotubes, and nanorods, are attracting much research interest because of their unique properties and many potential applications.[1−4] A large number of synthetic/fabrication methods are available for generating 1D nanostructures, including chemical synthesis,[5] electrochemical synthesis,[6] nanolithography,[7] and electrospining.[8] Compared with 1D nanostructures formed from metals, oxides, and semiconductors, the use of polymer nanofibers or nanowires may have several advantages because of their lightweight, lost cost, mechanical flexibility, and scalable production.[9] As a result, polymer nanofibers incorporating electrical, optical, and magnetic nanoparticles within hierarchal nanostructures have been prepared that exhibit multifunctional properties.[10−12]

Among inorganic materials, ZnO or ZnS nanoparticles are growing in technological importance because of their unique properties and applications, ranging from surface acoustic wave filters, photonic crystals, light-emitting diodes, photodetectors, optical modulator waveguides, and gas sensors.[13−15] Thus, combining the properties of 1D nanostructures with those of ZnO or ZnS polymer composites is an attractive prospect for the development of useful new materials.

In this paper, we report the preparation of organic metal salt [zinc dimethacrylate, $Zn(MA)_2$] nanofibers through self-assembly in organic solvents (methanol, ethanol, acetone, and THF) mixed with water. These monomeric $Zn(MA)_2$ nanofibers are converted into ZnO or ZnS nanoparticle/polymer nanofiber composites through a combination of γ-irradiated polymerizations and in situ thermal decomposition or H_2S gas/solid reactions, respectively. The $Zn(MA)_2$ monomer is used widely in golf balls and in food packing materials because after polymerization it exhibits reversible thermal behavior and strong mechanical properties through ionic bonding.[16] To maintain the morphologies of the $Zn(MA)_2$ monomeric nanofibers in the polymer nanocomposite, the $Zn(MA)_2$ can be polymerized through γ-irradiation in the solid state and then subjected to postcuring at 90 °C.[17]

Scheme 1 displays the synthetic pathway followed for the preparation of the ZnO and ZnS nanoparticle/polymer composite nanofibers. $Zn(MA)_2$ powder was first suspended in absolute ethanol to form a colloidal solution; the $Zn(MA)_2$ molecules were then self-assembled into nanofibrous supramolecular structures upon the addition of a suitable amount of water. These monomeric $Zn(MA)_2$ nanofibers were polymerized, forming poly(zinc dimethacrylate) [P-$Zn(MA)_2$] nanofibers, through a combination of ^{60}Co γ-ray irradiation and postcuring at 90 °C.[17] The ZnO, ZnS, and ZnO/ZnS nanoparticles were then generated from the P-$Zn(MA)_2$ nanofibers in situ through (i) exposing them to air at a temperature of 180 °C, (ii) performing H_2S gas/solid reactions at room temperature,[11] and (iii) sequentially exposing them in air at 180 °C for five hours and then performing the H_2S gas/solid reaction at room temperature, respectively. Furthermore, new and enhanced properties are expected due to confinement in nanoscale dimensions when controlled nanocrystalline forms of this system are developed. The development of ZnO and ZnS in its nanoparticle/polymer nanofibers nano-

* To whom correspondence should be addressed. E-mail: kuosw@faculty.nsysu.edu.tw (S.-W.K.); changfc@mail.nctu.edu.tw (F.-C.C.). Fax: 886-7-5254099 (S.-W.K.); 886-3-5131512 (F.-C.C.).
† National Sun Yat-Sen University.
‡ National Chiao Tung University.
§ Chonbuk National University.

10.1021/jp805156t CCC: $40.75
Published on Web 09/25/2008

SCHEME 1: Synthetic Pathway for the Preparation of ZnO or ZnS Nanoparticle/Polymer Composite Nanofibers

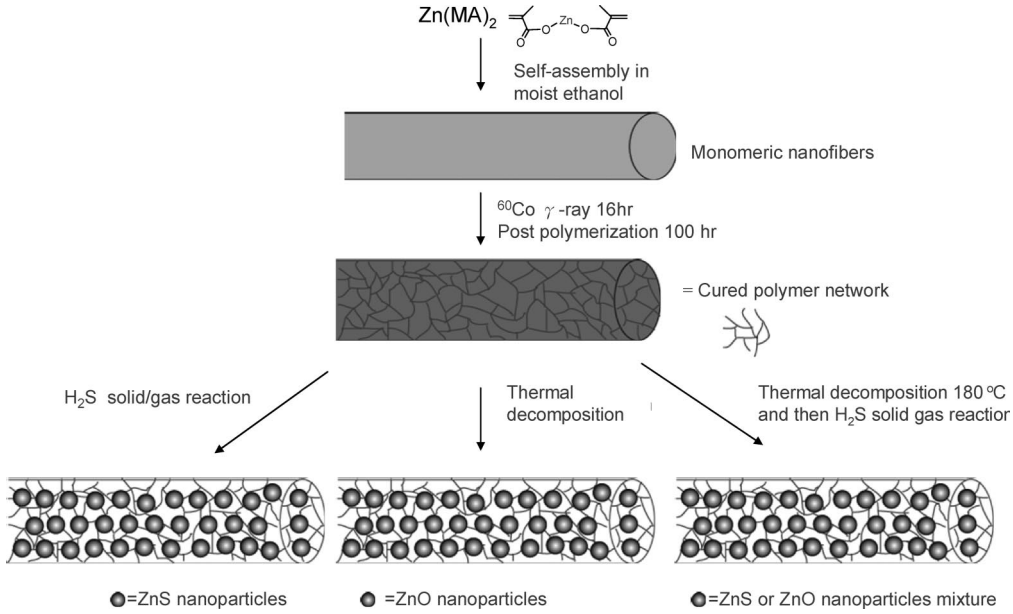

composite form and its successful integration into current and future device technologies is one of the goals of our research.

Experimental Section

Preparation of Hierarchical ZnO/ZnS Nanoparticle/Polymer Nanofiber. The $Zn(MA)_2$ (Aldrich) monomeric fibrous gel was prepared by suspending $Zn(MA)_2$ (0.1 g) in absolute ethanol (9.5 mL) and then adding water (0.5 mL) into the $Zn(MA)_2$ colloidal suspension. Complete gels typically formed within 30 min. The cross-linked $Zn(MA)_2$ nanofibers [P-$Zn(MA)_2$] were synthesized using the method developed by Parrish et al.[17] $Zn(MA)_2$ nanofibers were subjected to γ-ray irradiation at a dose rate of 6.493 kGy/h in the field of a ^{60}Co γ-ray source (2.9×10^4 Ci) for 16 h at room temperature. Thereafter, the samples were postpolymerized at 90 °C for 100 h. The ZnO and ZnS nanoparticle/polymer composite nanofibers were synthesized through thermal decomposition at 180 °C and H_2S solid/gas reactions, respectively.

Characterization. Thermal analyses were performed using a DuPont DSC-9000 differential scanning calorimeter operated at a scan rate of 20 °C/min within the temperature range from 30 to 220 °C. The thermal stabilities of the cured samples were investigated using a Du Pont 2050 TGA instrument operated at a heating rate of 10 °C/min from 30 to 700 °C under a nitrogen flow. Infrared spectra were recorded using a Nicolet Avatar 320 FTIR spectrophotometer; 32 scans were collected at a spectral resolution of 1 cm^{-1}. All samples were prepared under a continuous nitrogen flow to ensure minimal degrees of sample oxidation or degradation. A Hitachi S-4700I field emission scanning electron microscope (SEM) operated at 15 kV was employed to obtain SEM images of the nanofibers. Transmission electron microscopy (TEM) images and selected-area electron diffraction (SAED) patterns were obtained using a JEOL JEM-1200CX II transmission electron microscope operated at 120 kV. Specimens of the nanofibers were ultramicrotomed using a diamond knife on a Leica ultracut UCT to obtain thick films (thickness: ca. 700 Å). Subsequently, these films were placed on a 200 mesh copper net, and a layer of carbon (thickness: ca. 3 nm) was deposited for TEM observation. X-ray diffraction (XRD) data were collected on a MacScience M18XHF-SPA diffractometer using a Cu target radiation source (Cu Kα λ = 0.154 nm). Photoluminescence (PL) spectra were recorded using a Jobin−Yvon Spex Fluorolog-3 fluorescence spectrometer.

Results and Discussion

Figure 1a presents an SEM image of the $Zn(MA)_2$ monomeric nanofibers in moisture ethanol. We observe a random 3D flexible nanofiber network with fiber diameters of 100−200 nm and lengths ranging from tens to hundreds of micrometers, similar to the morphology with the polymer nanofibers formed through electrospinning.[18] Many low-molecular-mass gelators form supramolecular structure through self-assembly by noncovalent interactions to provide 3D networks that favor the gelation of a solvent.[19] A zinc complex having a carboxylate structure similar to that of $Zn(MA)_2$ forms a hydrogen-bonded framework structure in moist ethanol. We suspected that water clusters formed around the $Zn(MA)_2$ would undergo hydrogen-bonding interactions to create a supramolecular structure. Figure 1b displays a photograph of the $Zn(MA)_2$ colloidal anhydrous ethanol solution, which was transparent because the suspended $Zn(MA)_2$ particles were quite small ca. 10 nm by SAXS and TEM analysis (for brevity, data not shown here). After dropping a suitable amount of water (ca. 3−5 wt %), the colloidal solution became cloudy as shown in Figure 1c. Figure 1d shows the corresponding TEM image of Figure 1c obtained after freeze-drying the $Zn(MA)_2$ colloidal moisture ethanol solution and reveals that aggregation of ca. 10 nm nanoparticles led to the construction of 3D nanofibers, which then formed random networks after solvent evaporation as shown in Figure 1a. The 3D interconnecting fiber network could entrap large amounts of solvent, principally through capillary forces or surface tension, to form a gel. It was difficult to redissolve this metastable transient gel in water and ethanol, even under sonication.

Figure 2 presents the in situ FTIR spectra of $Zn(MA)_2$ recorded at various temperatures casting from moisture ethanol solution. Clearly, free hydroxyl absorption at 3610 cm^{-1}, dimmer hydroxyl-hydroxyl absorption at 3570 cm^{-1}, and multimer hydroxyl-hydroxyl absorption at 3420 cm^{-1} were observed where these peaks decrease with increasing temperature. These spectra support the notion of hydrogen bonding occurring between water molecules and $Zn(MA)_2$ units at room

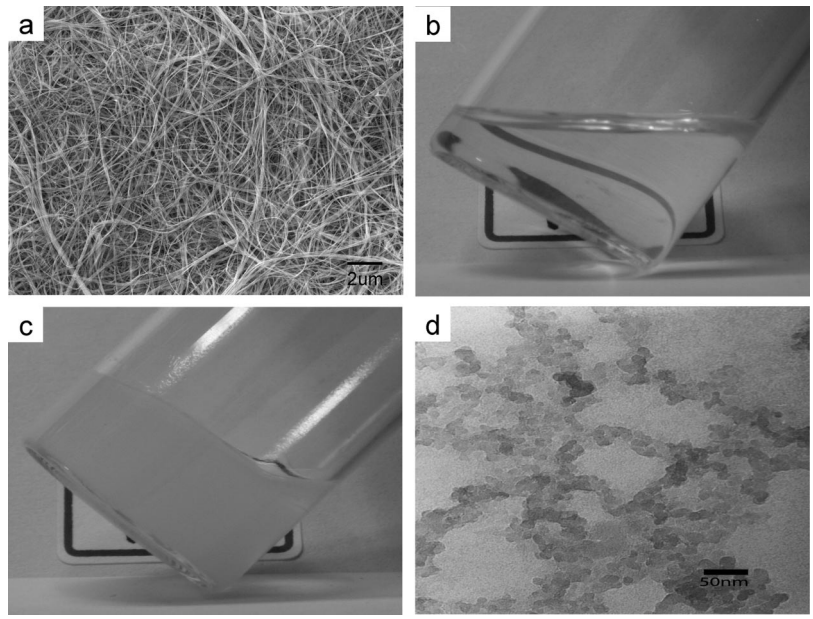

Figure 1. (a) SEM image of $Zn(MA)_2$ in moisture ethanol, (b) photograph of $Zn(MA)_2$ in anhydrous ethanol, (c) photograph of $Zn(MA)_2$ in moisture ethanol, and (d) TEM image of $Zn(MA)_2$ in moisture ethanol under freeze-drying.

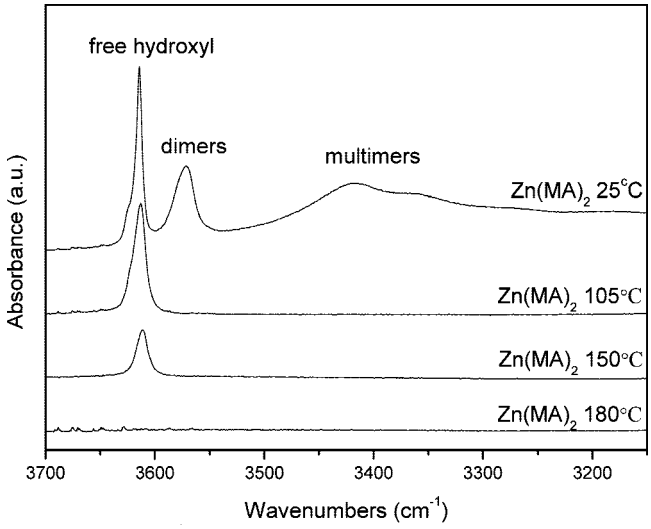

Figure 2. Partial FTIR spectra (3150−3700 cm^{-1}) of $Zn(MA)_2$ monomeric nanofibers recorded at room temperature, 105, 150, and 180 °C.

temperature and then form colloidal hydrated zinc salt and partially condensed zinc hydroxides.

Figure 3a depicts the possible chemical structure of $Zn(MA)_2$ in moisture ethanol solution. The corresponding TEM image of a freeze-dried $Zn(MA)_2$ sample prepared in ethanol/water as shown in Figure 3b reveals that the nanofibers formed through aggregation of colloid particles. Figure 3c provides a cartoon representation of the possible mechanism of nanofiber formation. Here, we also choose different organic solvents to prepare the $Zn(MA)_2$ nanofiber for comparison. Figure 4 displays SEM images of $Zn(MA)_2$ fibers formed in various water/organic solvent mixtures (methanol, acetone, and THF). Similarly, these images also display that $Zn(MA)_2$ can self-assemble into nanofiber patterns in different polar organic solvents. Therefore, water molecule plays an important role on the $Zn(MA)_2$ nanofiber formation in organic solvents.

Each $Zn(MA)_2$ monomer in the nanofibers contained two polymerizable acrylate units; therefore, cross-linked structures could be formed to enhance the mechanical strength and the thermal and chemical stability of the polymer nanofibers.[11] Because of the low conversion of either γ-irradiation or thermal polymerization of $Zn(MA)_2$ monomers,[17] we employed both γ-irradiation method and postpolymerization casting at a temperature of 90 °C [i.e., below the melting temperature (>200 °C) of $Zn(MA)_2$] to convert the $Zn(MA)_2$ monomeric nanofibers into P-$Zn(MA)_2$ polymeric nanofibers without altering their morphology. Figure 5a shows the FTIR spectroscopic analysis, revealing that the intensity of the normalized peak at 3090 cm^{-1} [corresponding to the C−H stretching vibration of the olefinic units of $Zn(MA)_2$] decreased upon increasing the postpolymerization time, implying that the combination of γ-irradiation and postpolymerization was an effective means of curing $Zn(MA)_2$ nanofibers in the solid state. From a comparison of the intensities of the signals for C−H stretching before and after postpolymerization for 100 h, we calculated the degree of conversion to be ca. 40% as shown in Figure 5b. The resulting P-$Zn(MA)_2$ nanofibers were stable in most organic solvents, as indeed were the precursor $Zn(MA)_2$ nanofibers. Figure 6a provides TGA traces of both the $Zn(MA)_2$ monomeric and P-$Zn(MA)_2$ nanofibers. We observe that after polymerization, the P-$Zn(MA)_2$ nanofibers show relative lower monomer content, higher char yield, and an improvement of thermal properties compared to $Zn(MA)_2$. The glass transition temperature of P-$Zn(MA)_2$ is 105 °C, which is similar to that of poly(methyl methacrylate, PMMA) as shown in Figure 6b. The ionic bonding of zinc ion could enhance glass transition temperature significantly; however, only 40% degree of conversion of P-$Zn(MA)_2$ would decrease the Tg because of 60% monomers that are used as the diluent to increase the free volume. As a result, the P-$Zn(MA)_2$ shows the similar Tg behavior with PMMA. The SEM image of the sample after polymerization (Figure 6d) reveals that no obvious morphological change occurred during the polymerization process compared with Figure 6c, that is, $Zn(MA)_2$ nanofibers can be polymerized without causing significant structural damage.

The zinc ions [27.8 wt % in P−$Zn(MA)_2$ nanofibers] act as nucleation sites in the polymer chains for further formation of densely dispersed functional ZnO or ZnS quantum dots within the polymer nanofibers. We prepared the ZnO quantum dots in

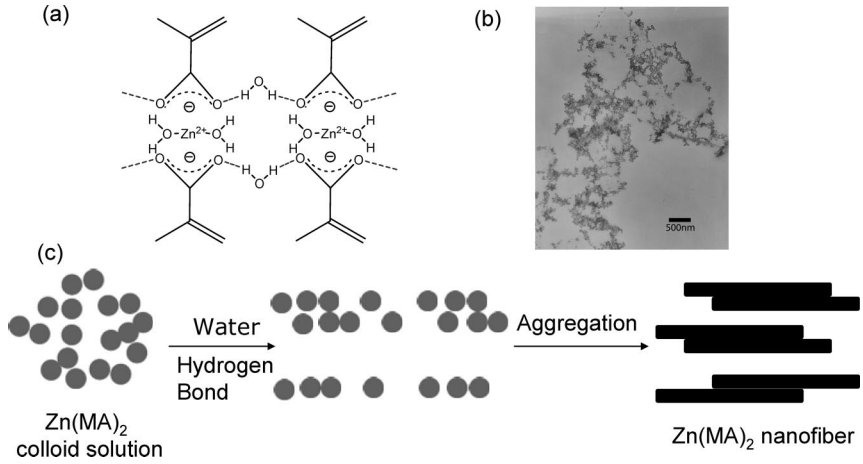

Figure 3. (a) Schematic representation of the hydrogen bonding array formed from zinc methacrylate and water. (b) TEM image of a freeze-dried $Zn(MA)_2$ sample that had self-assembled in ethanol/water. (c) A possible mechanism for nanofiber formation.

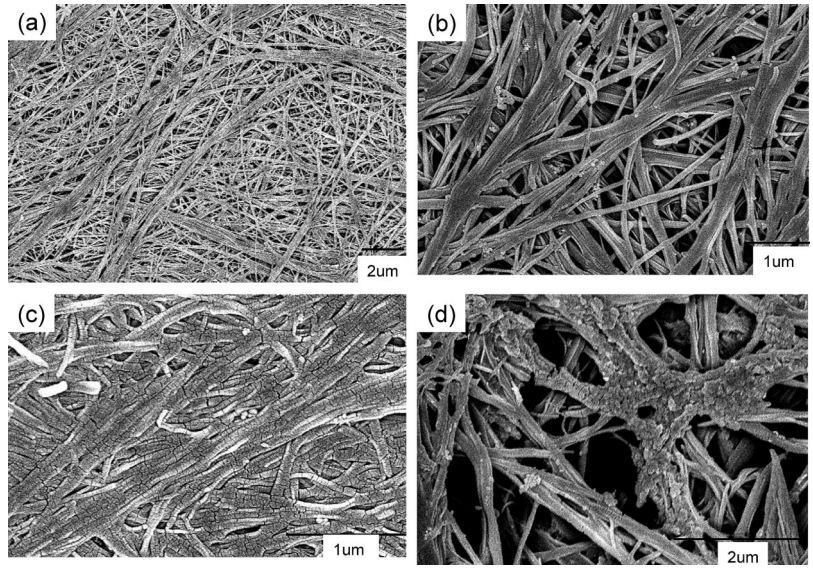

Figure 4. (a) SEM image of $Zn(MA)_2$ self-assembled in water/methanol. (b) Scale-expanded image of panel a. (c,d) SEM images of $Zn(MA)_2$ self-assembled in (c) water/acetone and (d) water/THF.

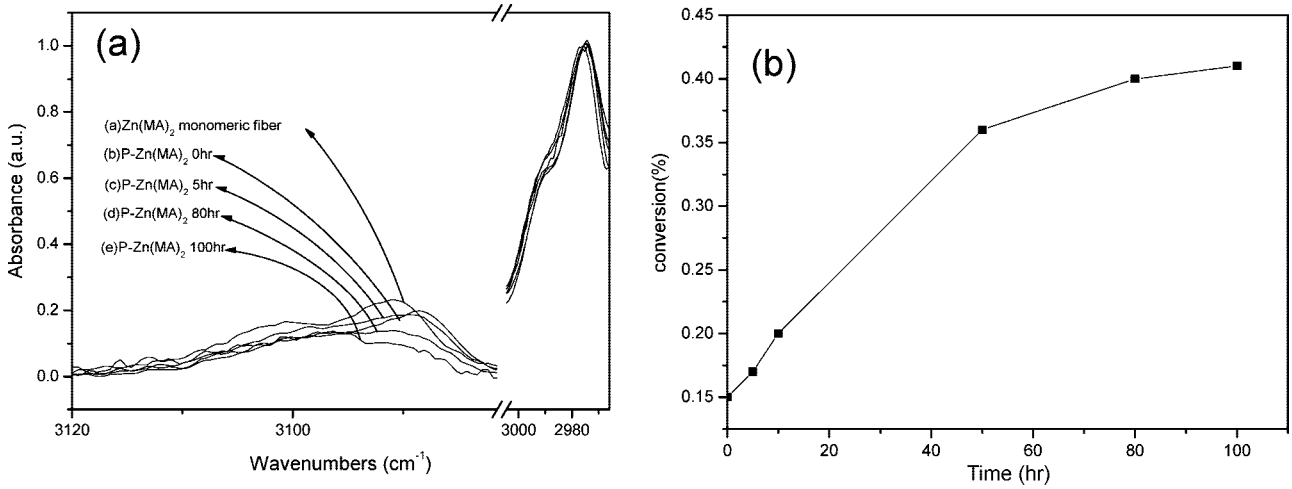

Figure 5. (a) FTIR spectra of $Zn(MA)_2$ after γ-irradiation for postcuring at 90 °C for various lengths of time. (b) Conversion of polymerization for postcuring at 90 °C for various lengths of time.

situ by thermal condensation with the P-$Zn(MA)_2$ nanofibers in hot air (180 °C) for different hours, obtaining ZnO quantum dot/polymer composite nanofibers [P-$ZnO(MA)_2$]. In the case of the ZnO nanoparticles, we investigated the transformation of the zinc ions in the P-$Zn(MA)_2$ nanofibers under thermal decomposition by monitoring the intensity of two significant peaks ($2\theta = 9.09, 10.78°$) in the P-$Zn(MA)_2$ nanofiber crystal structure. Figure 7a displays XRD patterns of the P-$ZnO(MA)_2$

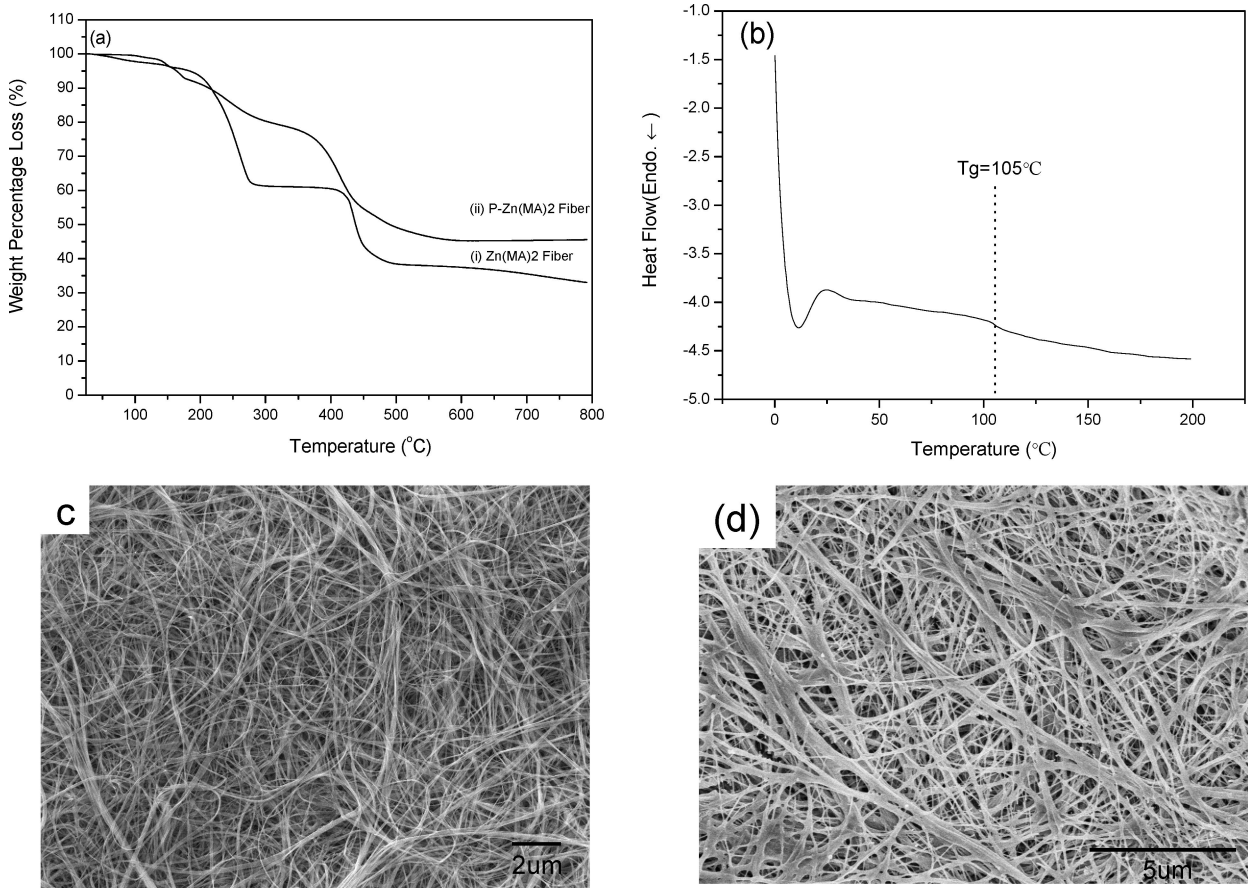

Figure 6. (a) TGA traces of $Zn(MA)_2$ monomeric nanofibers and P-$Zn(MA)_2$ nanofibers after polymerization; (b) DSC trace of P-$Zn(MA)_2$ nanofibers; (c) SEM image of $Zn(MA)_2$ monomeric nanofiber; (d) SEM of P-$Zn(MA)_2$ nanofiber.

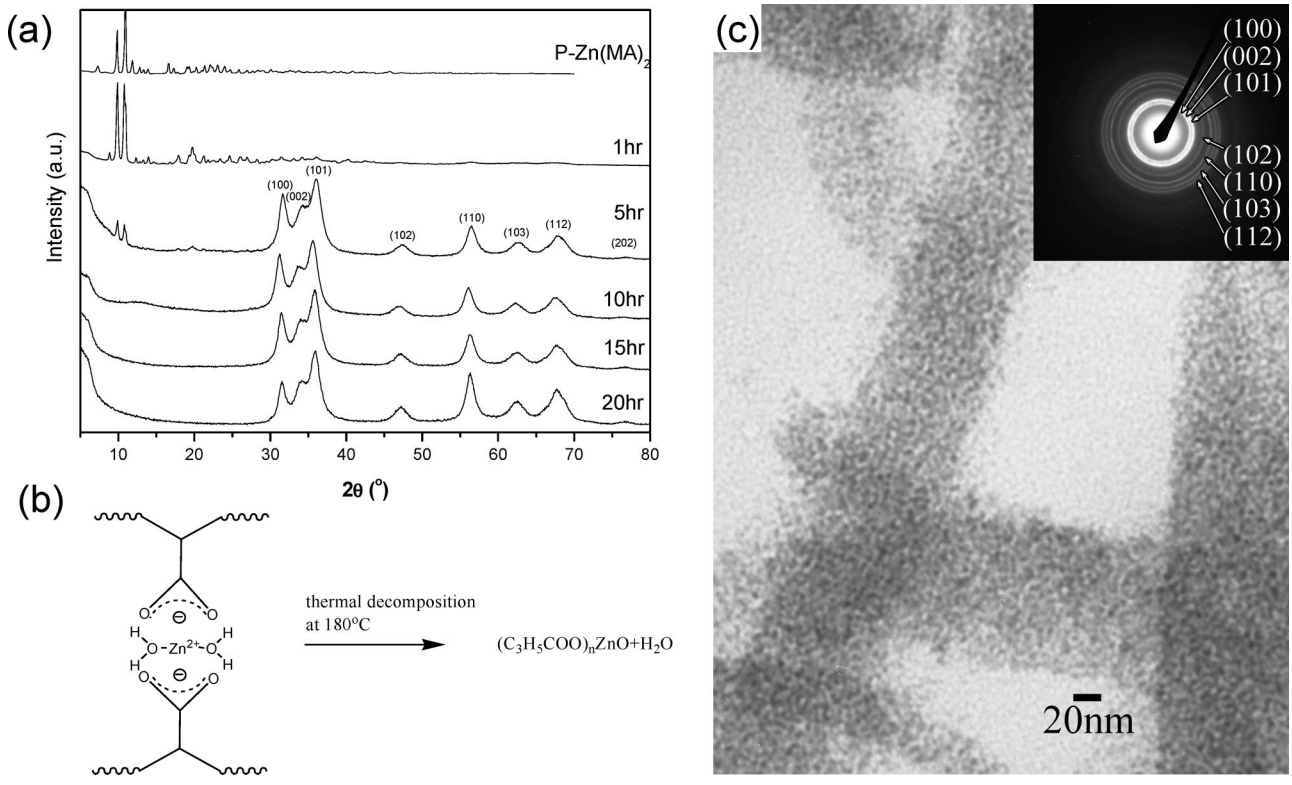

Figure 7. (a) XRD diffraction patterns of P-$Zn(MA)_2$ nanofibers oxidized at 180 °C for various periods of time; (b) the thermal decomposition mechanism of ZnO nanoparticle formation; (c) TEM image of the P-$ZnO(MA)_2$ nanofiber composite obtained after oxidation at 180 °C for 15 h.

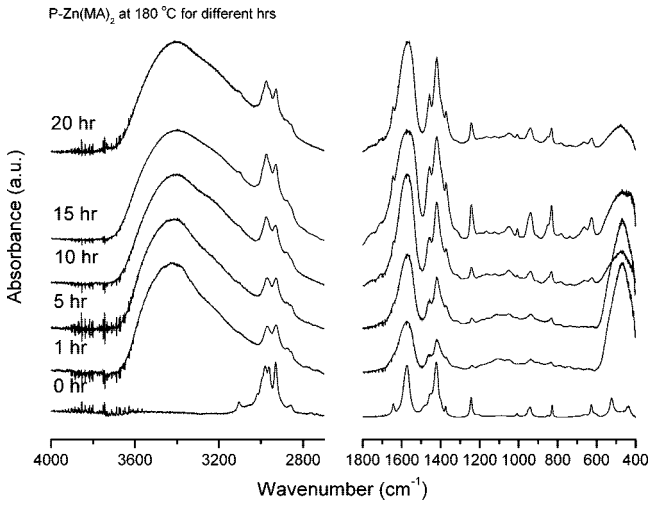

Figure 8. In-situ FTIR spectra of P-Zn(MA)$_2$ at 180 °C for various lengths of time.

and P-Zn(MA)$_2$ nanofibers subjected to thermal decomposition at 180 °C for various periods of time. After oxidation for 15 h, we observe no characteristic peaks for the P-Zn(MA)$_2$ nanofibers, indicating P-Zn(MA)$_2$ precursor could be transformed into crystalline ZnO at temperatures as low as 180 °C. Indeed, we observed diffraction peaks corresponding to the (110), (002), (101), (102), (110), (103), and (112) planes of hexagonal ZnO nanoparticles after only 5 h of oxidation.[14] The mean size of the ZnO nanocrystallites, determined using Scherrer's formula,[20] was ca. 7.73 nm after thermal decomposition at 180 °C for 15 h. The zinc ions in the P-Zn(MA)$_2$ crystals were thermally condensed individually; these very small nanoparticles were nucleated in the lattices during the initial stages of the reaction. After longer periods of thermal condensation, the nanoparticles that formed tended to aggregate to form larger particles through Oswald ripening. Furthermore, the crystalline lattices of the fibers served as matrices that prevented the ZnO nanoparticles from growing too large. Because the ZnO nanoparticles remained complexed to the methacrylate groups in the nanofibers as shown in Figure 7b, the morphology of the fibers remained relatively unchanged during the in situ generation of the ZnO nanoparticles. The TEM image of the composite nanofibers in Figure 7c reveals a dense set of ZnO nanoparticles having diameters of ca. 7∼8 nm that were separated from one another and well dispersed within the polymer nanofibers. The SAED pattern (inset to Figure 7c) was in accordance with the results of X-ray diffraction patterns (Figure 7a). The mechanical properties and cross-linked networks formed by the polymer units in the composite nanofibers not only strengthened the morphology of the nanofibers but also enhanced the stability of the immobilize ZnO nanoparticles.

Figure 8 shows corresponding in situ FTIR measurement of P-Zn(MA)$_2$ nanofibers exposing at 180 °C for different hours. Clearly, P-Zn(MA)$_2$ at 180 °C for the initial sample did not show any hydroxyl stretching absorption. On the basis of the chemical reaction in Figure 7b, the colloidal hydrated zinc salts and partially condensed zinc hydroxides formed upon the addition of water undergo a thermal condensation to zinc oxide. With the increase of thermal decomposition time, the hydroxyl-stretching, ranging 3200−3700 cm^{-1}, corresponds to the multimer hydrogen-bonded hydroxyl group (H_2O molecule) and the ZnO-related vibration peak locates at 500 cm^{-1}, which is a significant increase, confirming the formation of the thermal condensation ZnO nanoparticle. In general, the carbonyl group (C═O) and C−O stretching are located at 1730 and 1150 cm^{-1}, respectively. Acrylic groups consist of a mixture of unidentate, chelate, and bridging type structures with zinc ions, resulting in different position peaks at C═O (1550−1600 cm^{-1}) and C−O (1400−1460 cm^{-1}) vibrations.[21−23] Thus peaks at 1570 cm^{-1} and 1420 cm^{-1} are assigned to carboxylic ionic complex and C−O stretching vibration of the carbonyl group of Zn(MA)$_2$·2H$_2$O and peaks at 1643 and 1457 cm^{-1} are assigned to the C═O and C−O stretching vibrations of acrylate group on the surface of ZnO nanoparticle, while peaks at 1370 and 1040 cm^{-1} relate to some complex structure of the COO$^-$ group with zinc ion, which can be called carboxylic ionic complex. As a result, we can conclude that ZnO nanoparticle in P-Zn(MA)$_2$ is chemisorbed by the carboxylic group from the hydrolization of the partial ester group by OH$^-$ as shown in Figure 7b. The methacrylate group plays a significant role during the synthesis of ZnO nanoparticles. In the thermal condensation process, the nucleation of particles is a complicated process.[24] The ionization group of RCOO$^-$ in P-Zn(MA)$_2$ can directly interact with the positive charged zinc atoms to generate chemisorbed polymer on the surface of ZnO nanoparticles. Because of RCOO$^-$ group to ZnO nanoparticles, P-Zn(MA)$_2$ restricts the growth of the ZnO nanoparticles (ca. 7∼8 nm based on HRTEM). While in the absence of polymers, ZnO nanoparticles always grow uncontrolled far beyond the size range.[25]

In addition, we also prepared ZnS quantum dots in situ by exposing the P-Zn(MA)$_2$ nanofibers to H_2S at room temperature. Figure 9a,b displays SEM images of P-ZnS(MA)$_2$; again, the nanofibers were not destroyed during the reaction with H_2S. The TEM image of the ZnS nanoparticle/polymer composite nanofibers in Figure 9c reveals that dense ZnS nanoparticles having diameters of ca. 3−4 nm were separated from one another and well dispersed in the polymer nanofibers, presumably because some of the carboxyl units remained bonded to zinc ions on the particles' surfaces after the reaction with H_2S. The compact polymer network prevented the ZnS nanoparticles from aggregating, which is similar to the ZnO system. The SAED pattern (inset to Figure 9c) reveals that the ZnS nanoparticles had cubic crystal structures, which was in accordance with the result of X-ray diffraction as shown in Figure 9d. The presence of diffraction peaks corresponding to the (111), (220), and (311) planes indicates that the ZnS nanoparticles in the nanofibers possessed zinc blende crystal structures.[13] The crystal structure in the P-Zn(MA)$_2$ was quite different from that in P-ZnS(MA)$_2$, implying that almost all of the zinc ions were transformed into ZnS nanoparticles during the H_2S solid/gas reaction.

In addition, when we performed the oxidation for only 5 h and then subjected the sample to the H_2S solid/gas reaction, we obtained a ZnO/ZnS nanoparticle mixture. Figure 10a indicates that the X-ray diffraction patterns of both ZnO and ZnS crystals were present. Figure 10b,c presents SEM and TEM images of the mixed ZnO/ZnS nanoparticles in the polymer nanofiber composites; again, the ZnO/ZnS nanoparticle mixtures were well dispersed.

Because our synthesized ZnO, ZnS, and ZnO/ZnS, nanoparticles were all quantum-sized semiconductor nanoparticles, we measured the photoluminescence (PL) spectra of these various quantum dot/polymer composites. Figure 11 displays the room-temperature PL spectra of these nanofiber composites. The strongest PL emissions appeared at 475−490 nm with excitation wavelengths at 397−409 nm, indicating that our synthesized quantum dots are wide-bandgap semiconductor nanoparticles exhibiting blue emission properties.

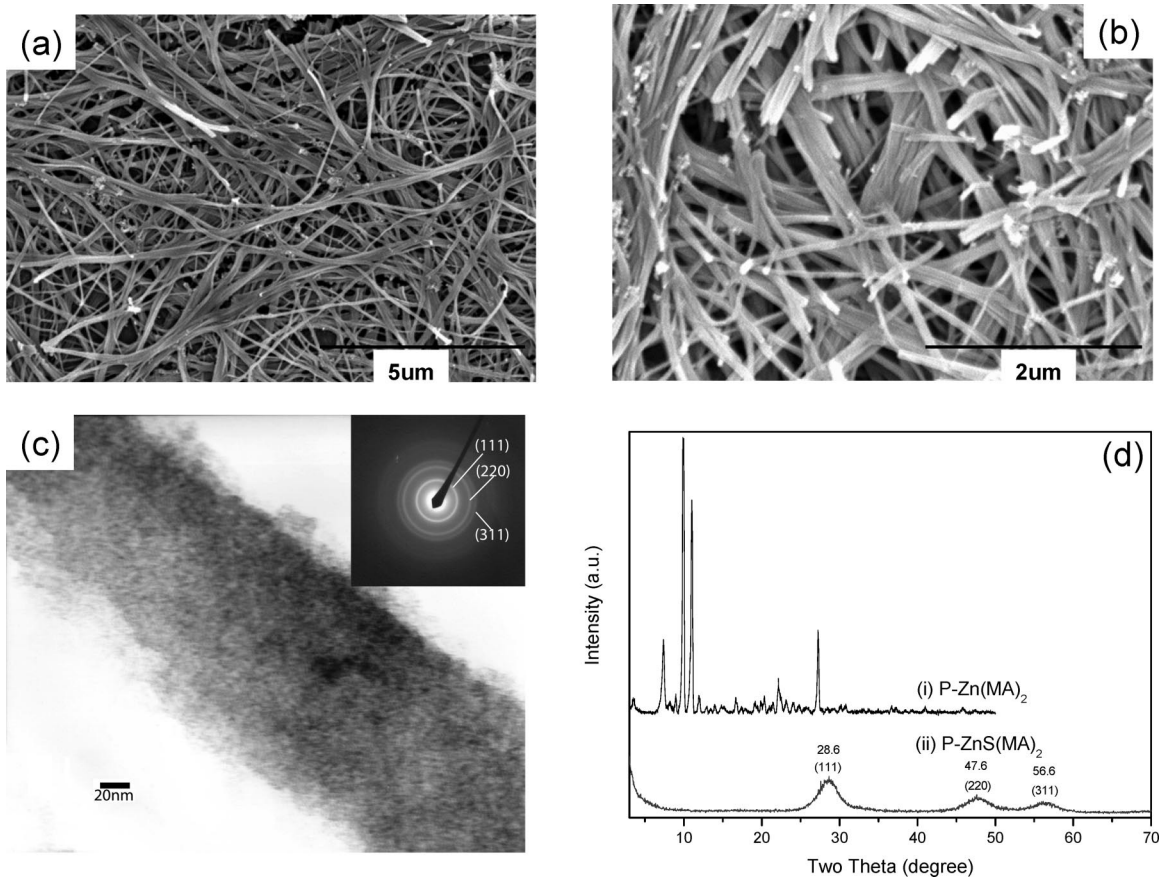

Figure 9. (a) SEM image of P-ZnS$(MA)_2$ nanofiber composite; (b) scale-expanded image of panel a; (c) TEM image and SAED pattern of P-ZnS$(MA)_2$ nanofiber composite; (d) X-ray diffraction patterns of P-Zn$(MA)_2$, and P-ZnS$(MA)_2$ nanofibers.

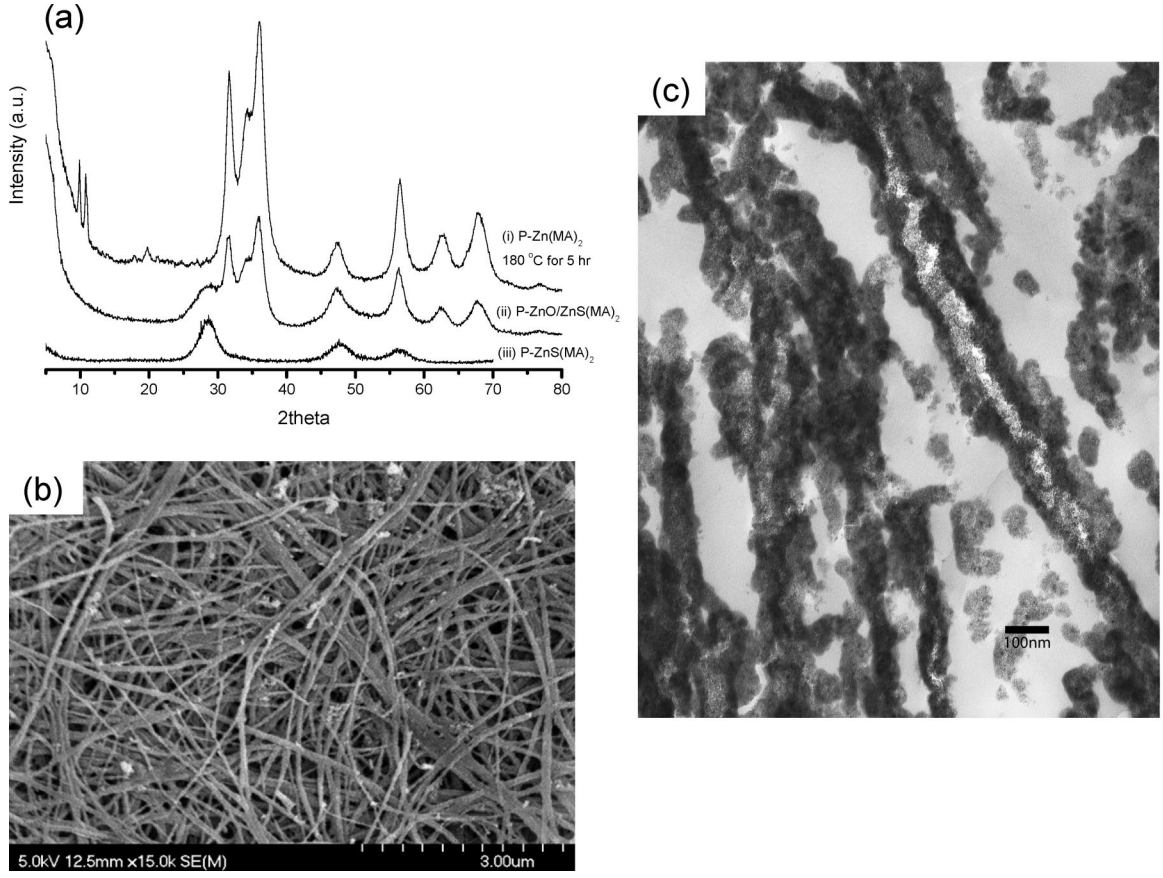

Figure 10. (a) XRD diffraction patterns of the P-ZnO$(MA)_2$, P-ZnO/ZnS$(MA)_2$, and P-ZnS$(MA)_2$ nanofibers; (b) SEM image of the P-ZnO/ZnS$(MA)_2$ nanofibers; (c) TEM image of the P-ZnO/ZnS$(MA)_2$ nanofibers.

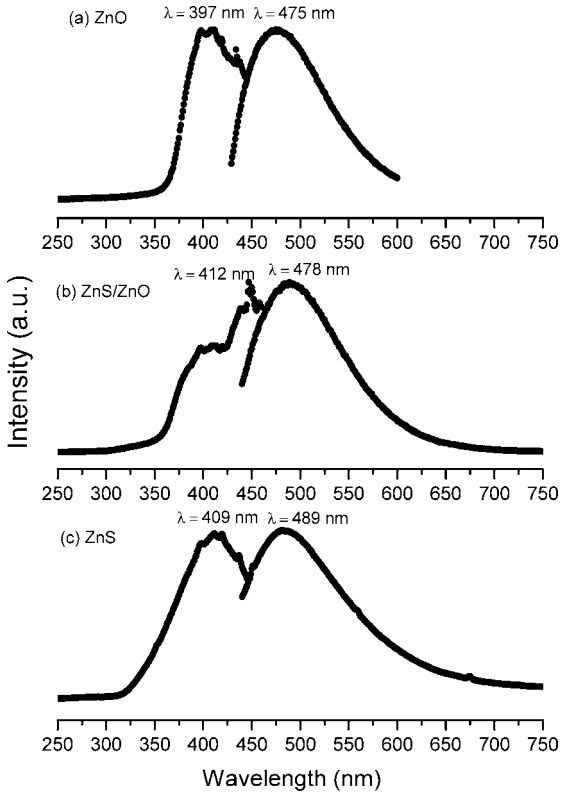

Figure 11. PL spectra of the ZnO, ZnS/ZnO, and ZnS quantum dot/polymer composite nanofibers (excitation at 397, 412, and 409 nm, respectively).

Conclusions

In summary, we have developed a novel, simple technique for fabricating both ZnO and ZnS quantum dot/polymer composite nanofibers through a combination of γ-irradiation, postpolymerization, and either thermal oxidations or H_2S solid/gas reactions. The fine and highly crystallized ZnO and ZnS nanoparticles were modified by carboxylic ionic complexes, which are from the self-assembly behavior of zinc dimethyl methacrylate in moisture organic solvents. ZnO and ZnS nanoparticles emit UV located at 397∼407 nm originated from the quantum size effect, and the PL peak at 475∼490 nm originated from bound excitons in R−(COO)−ZnO and R−(COO)−ZnS complexes. This method represents a simple approach to produce nanostructured ZnO and ZnS in polymer nanofibers. This preparation method can be potentially extended to other poly(dimethacrylate) matrices containing the different metal ions.

Acknowledgment. This work was supported financially by the National Science Council, Taiwan, Republic of China, under Contract No. NSC-96-2120-M-009-009 and NSC-97-2221-E-110-013-MY3.

References and Notes

(1) Xia, Y.; Yang, P.; Sun, Y.; Wu, Y.; Mayers, B.; Gates, B.; Yin, Y.; Kim, F.; Yan, H. *Adv. Mater.* **2003**, *15*, 353.
(2) Xiong, Y.; Mayers, B. T.; Xia, Y. *Chem. Commun.* **2005**, 5013.
(3) Hurst, J.; Payne, E. K.; Qin, L.; Mirkin, C. A. *Angew. Chem., Int. Ed.* **2006**, *45*, 2672.
(4) Duan, X. F.; Huang, Y.; Cui, Y.; Wang, J. F.; Lieber, C. M. *Nature* **2001**, *409*, 66.
(5) Haung, J. X.; Kaner, R. B. *J. Am. Chem. Soc.* **2004**, *126*, 851.
(6) Mieszawaka, A. J.; Jalilian, R.; Sumanasekera, G. U.; Zamborini, F. P. *Small* **2007**, *3*, 722.
(7) Chou, S. Y.; Krauss, R. P.; Renstrom, P. J. *Science* **1996**, *272*, 85.
(8) Wang, X.; Drew, C.; Lee, S. H.; Senecal, K. J.; Kumar, Y.; Samuelson, L. A. *Nano Lett.* **2002**, *2*, 1273.
(9) Hou, H. Q.; Reneker, D. H. *Adv. Mater.* **2004**, *16*, 69.
(10) Zhang, L. J.; Wan, M. M. *J. Phys. Chem. B* **2003**, *107*, 6748.
(11) Cui, T.; Cui, F.; Zhang, J.; Wang, J.; Huang, J.; Lu, C.; Chen, Z.; Yang, B. *J. Am. Chem. Soc.* **2006**, *128*, 6298.
(12) Schlecht, S.; Tan, S.; Yosef, M.; Dersch, R.; Wendorff, J. H.; Jia, Z.; Schaper, A. *Chem. Mater.* **2005**, *17*, 809.
(13) Lu, C.; Cheng, Y.; Liu, Y.; Liu, F.; Yang, B. *Adv. Mater.* **2006**, *18*, 1188.
(14) Vayssieres, C. *Adv. Mater.* **2003**, *15*, 464.
(15) Hu, J. Q.; Bando, Y.; Zhan, J. H.; Golberg, D. *Angew. Chem., Int. Ed.* **2004**, *43*, 4606.
(16) Charara, Z. N.; Williams, J. W.; Schmidt, R. H.; Marshall, M. R. *J. Food Sci.* **1992**, *57*, 963.
(17) Parrish, C. F.; Kochanny, G. L. *Makromol. Chem.* **1968**, *115*, 119.
(18) Li, D.; Xia, Y. *Adv. Mater.* **2004**, *16*, 1151.
(19) Terech, P.; Sangeetha, N. M.; Maitra, U. *J. Phys. Chem. B* **2006**, *110*, 15224.
(20) Cullity, B. D. *Elements of X-Ray Diffractions*; Addison-Wesley: Reading, MA, 1978; p 102.
(21) Tokumoto, M. S.; Briois, V. *J. Sol-Gel Sci. Technol.* **2003**, *26*, 547.
(22) Sakohara, S.; Ishida, M.; Anderson, M. A. *J. Phys. Chem. B* **1998**, *102*, 10169.
(23) Pandiarajan, S.; Unadevi, M.; Sasirekha, V.; Rajaram, R. K.; Ramakrishnan, V. *J. Raman Spectrosc.* **2005**, *36*, 950.
(24) Boukari, H.; Lin, J. S.; Harris, M. T. *Chem. Mater.* **1997**, *9*, 2376.
(25) Cozzoli, P. D.; Curri, M. L.; Agostiano, A. *J. Phys. Chem. B* **2003**, *107*, 4756.

JP805156T